

# Characterizing Channel Fading in Vehicular Visible Light Communications with Video Data

Zhiyong Cui<sup>\*†</sup>, Chenqi Wang<sup>‡</sup>, and Hsin-Mu Tsai<sup>†‡</sup>

Department of Software and Microelectronics, Peking University, Beijing, China<sup>\*</sup>

Intel-NTU Connected Context Computing Center, Taipei, Taiwan<sup>†</sup>

Department of Computer Science and Information Engineering, National Taiwan University, Taipei, Taiwan<sup>‡</sup>

Email: 1201210546@pku.edu.cn, {r01922140,hsinmu}@csie.ntu.edu.tw

**Abstract**—There is no prior work in characterizing fading caused by vehicle mobility in vehicular visible light communications (V2LC). Different from a radio frequency (RF) communication link, the path loss of a V2LC link is dictated by not only the transmitter-receiver (T-R) distance, but also the irradiance angle and the incidence angle, which have large variation when the vehicles are in motion. In this paper, we took a novel approach to take a first look at the problem. Utilizing the video data obtained from a dashboard camera and computer vision techniques, we are able to estimate the relative location and angle parameters of neighboring vehicles with great level of detail. These parameters are then used to derive a time function of path loss, with which the autocorrelation and the channel coherence time are calculated. Our results show that V2LC links have much slower channel time variation compared to RF V2V links: the coherence time is at least an order larger.

**Index Terms**—Vehicular Visible Light Communication (V2LC), Visible Light Communications (VLC), Vehicle-to-Vehicle (V2V) Communications, Channel Fading.

## I. INTRODUCTION

Light Emitting Diode (LED) has become very common in automotive lighting in recent years, due to its superior safety performance (faster rise time compared to convention light sources), lower energy consumption, extreme vibration resistance, and smaller dimensions of its packaging. It is anticipated by 2015 the penetration of LED tail lights, brake lights, center high-mounted stop lights (CHMSL) will all be more than 50% [1]. Modulating these existing LED lights, such as the tail lights and the head lights of a vehicle, to transmit optical signals, Vehicular Visible Light Communications (V2LC) provides a reliable solution to implement vehicle-to-vehicle (V2V) communications [2] and requires minimum additional cost to install such a system. On the receiving end, V2LC utilizes either a photodiode module or a camera installed on a vehicle as the receiving component to obtain and to demodulate the transmitted optical signal.

In addition to lower cost, V2LC has many benefits compared to conventional radio frequency (RF) vehicular communications, such as Dedicated Short Range Communications (DSRC) [3]. It was shown that V2LC scales better in dense vehicle traffic; this is due to the fact that visible light can only propagate with line-of-sight (LOS) condition, and it significantly reduces the amount of interference received by each vehicle [2] and improves communication reliability. In addition, the line-of-sight only property of V2LC also provides

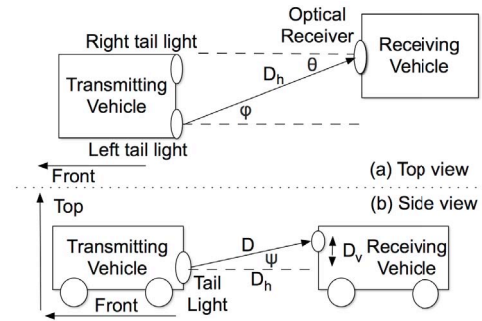


Fig. 1. System Model

stronger resistance to security threats in vehicular networks, as physically it is harder to inject traffic or to interfere with ongoing transmission without attracting attention. As a result, V2LC presents itself as a good technology candidate for bootstrapping the penetration of V2V communications, or a technology to complement RF V2V communications to provide better reliability and security.

Although there has been significant amount of work characterizing V2V RF channels, there is very little work investigating V2V VLC channels. Different from V2V RF channels, multipath propagation in V2V VLC channels is not significant, due to two reasons: (1) VLC modulates optical signal power; compared to RF communications, which modulates signal amplitude, the effective path loss is the square of the original path loss exponent. This means that the power of the multipath components are significantly reduced and these signal components can often be ignored. (2) Visual obstacles could block the propagation of many multipath components. Therefore, the most important aspects of the characterization of V2V VLC channels are related to large-scale fading: the *path loss model* [4] and *how the path loss (and hence the received power) vary over time*. In this paper, we will investigate the latter.

The path loss of a VLC link is dictated by the transmitter-receiver (T-R) distance, the irradiance angle, and the incidence angle. As a result, mobility of the vehicles while driven on the road, which changes all three of these parameters over time, is a major source of time variation of received power. Existing theoretical or simulation mobility models do not have

the level of detail required to carry out the study to characterize this time variation. In this paper, we take an experimental approach. Utilizing the video data collected from cameras mounted on driven vehicles, computer vision techniques are used to identify the location of the tail lights of neighboring vehicles (the transmitting vehicle) with respect to the host vehicle with the camera (the receiving vehicle). With the estimated location parameters of a single image, the path loss of the V2LC link between these two vehicles at that time instance can be estimated; performing the same operation over a series of images taken from a video, a time function of the V2LC path loss can be obtained. We then analyzed the obtained path loss functions to characterize the channel fading due to vehicle mobility. The main benefit of this approach is that it is possible to obtain a larger collection of data from a variety of different scenarios for better fidelity and the fact that it does not require an actual working V2LC measurement system. We consider this work as a pilot study to understand the severity of V2LC channel fading and whether further experimentation with the standard channel measurement approach is needed.

## II. SYSTEM MODEL

Fig. 1 shows the system considered in this study. The transmitting vehicle modulates both the left and the right tail lights to emit optical signal. The receiving vehicle is equipped with an optical receiver, which could be a photodiode module or a camera, mounted in the center of the front side of the vehicle.  $D_h$  is the horizontal distance between the transmitting tail light and the receiving optical component,  $D_v$  is the vertical distance due to the difference of heights of the transmitter and the receiver, and  $D = \sqrt{D_h^2 + D_v^2}$  is the actual distance between the transmitter and the receiver.  $\phi$  is the horizontal irradiance angle,  $\theta$  is the horizontal incidence angle, and  $\psi$  is the elevation angle. After considering  $\psi$ , the irradiance angle and the incidence angle are given by  $\phi' = \cos^{-1}\left(\frac{D_h \cos \phi}{D}\right)$  and  $\theta' = \cos^{-1}\left(\frac{D_h \cos \theta}{D}\right)$ , respectively. The path loss of a V2LC link is then given by

$$H(0) = \frac{(n+1)A_R}{2\pi D^\gamma} \cos^n(\phi') \cos(\theta') \quad , \quad (1)$$

where  $A_R$  is the optical detector area,  $\gamma$  denotes the optical path loss exponent, and  $n = -\frac{\ln 2}{\ln(\cos \Phi_{1/2})}$  is determined by the half-power angle  $\Phi_{1/2}$  of the transmitting LED source. The received optical power of a V2LC link is then given by

$$P_R = H(0)P_T \quad , \quad (2)$$

where  $P_T$  is the transmitting optical power.

The following describes our assumptions:

- Each tail light is assumed to have a single LED source and the output optical radiation follows a Lambertian radiation pattern. Although many LED tail lights utilize an array of LED chips, our earlier study [4] shows that the output radiation pattern of such a light can be well approximated with a piecewise Lambertian model with two sets of  $\gamma$  and  $\Phi_{1/2}$ . The measured values reported in [4] will be used in this study.

- In our study, we assume  $\phi = \theta$  as most of the time the vehicles are traveling toward the same direction.

## III. DATA COLLECTION AND VIDEO PROCESSING

The goal of the computer vision techniques presented in this section is to locate the tail lights of a vehicle in the images extracted from the video, and subsequently the incidence angle and the distance to the receiving vehicle can be estimated.

### A. Vehicle and Tail Light Detection

We design a three-step approach to perform tail light detection in complex daytime scenes with high precision:

- 1) **Vehicle detection** is performed on the entire image. The bounding box of a vehicle is obtained, and the tail lights should be located in this bounding box. We use a state-of-the-art object detection method that works well for pedestrian and vehicle detection - Deformable Part Model (DPM) [5]. This method can be characterized by three parts: (1) strong low-level features based on histograms of oriented gradients (HOG); (2) Efficient matching algorithms for deformable part based models in pictorial structures; (3) Discriminative learning with latent variables using latent support vector machine (SVM). We used PASCAL 2007 data set for cars as the training data set for this method. The method is proven to have high precision in detecting vehicles with different types, colors, and from different view angles (see Fig. 2 for an example).
- 2) **Tail light detection** is then performed with the image region within the bounding box(es) obtained from the previous step. Similar to a few existing methods [6], in this step we identify the pixels with red colors as the candidates of the tail lights. To allow better precision, we convert the images to HSV color space and set loose thresholds to obtain pixels ranging from pink-red to red-orange and including bright and dark red colors<sup>1</sup>. As we only perform detection in the bounding box provided by the previous step, a large portion of false detection can be avoided. We then utilize a density-based clustering method, Optics [7], to identify the two image regions with the largest density of red pixels, which usually correspond to the tail lights (see Fig. 3). If no such region or only one region is detected, the current image frame will not be considered for the subsequent location parameter estimation.
- 3) **Vehicle tracking** is then performed on series of image frames. For each image, we assign all detected vehicles with two detected tail lights a vehicle ID number. All collected video has a frame rate of 30 frame per second (fps). As in 1/30 second the location of the vehicle and its tail lights in the image will not change drastically, we choose to track the vehicle using a simple approach, described as follows. If the X coordinate of the centroid of a detected vehicle in the new image frame falls

<sup>1</sup>The thresholds used: hue:  $331^\circ - 20^\circ$ ; saturation: 0.2 - 1; value: 0.05 - 1.



Fig. 2. Vehicle detection by DPM

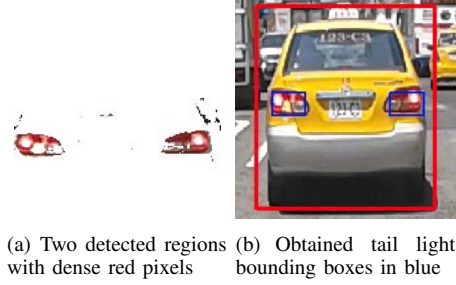


Fig. 3. Tail light detection by OPTICS

between respectively the left and the right boundaries of the detected left and right tail lights of a detected vehicle in the previous  $N$  image frames, then the detected vehicle in the new image frame will be considered as the same vehicle in one of the previous  $N$  image frames and given the same vehicle ID number. If there are multiple candidates satisfying this criterion, then the one that satisfies the criterion for the largest number of times in these  $N$  image frames will be chosen.

### B. Location Parameter Estimation

This subsection describes the method used to estimate various parameters needed to calculate the path loss  $H(0)$ , including  $D$ ,  $D_h$ ,  $\phi$ , from the size and the location of the detected tail light in the images. Fig. 4 shows various image parameters used in the calculation. The uppercase symbols (e.g.,  $W_R$ ) denote the distances in reality while the lowercase symbols (e.g.,  $w_R$ ) denote the distances in the image in unit of pixel. We first obtain a ratio between the actual distance and the distance in the image,  $\epsilon$ , given by

$$\epsilon = \frac{W_B}{w_B}, \quad (3)$$

where  $w_B$  and  $W_B$  are the distances between the left boundary of the left tail light and the right boundary of the right tail light in the image and in reality, respectively. The value of  $W_B$  is assumed to be 1.57 m, based on an assumption that the average width of a car is 1.7 m. Then the length of the projection of the T-R distance on the perpendicular axis out of the receiver (see Fig. 4) can be given by

$$D_p = \frac{x_{\max}}{2} \epsilon \tan\left(\frac{\Phi}{2}\right). \quad (4)$$

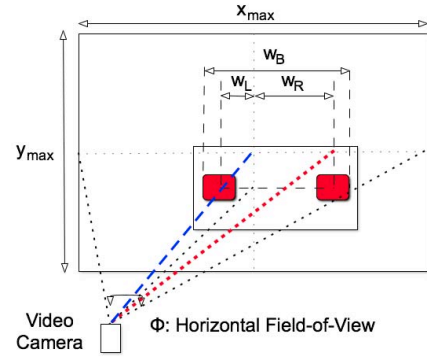


Fig. 4. Image parameters used in location parameter estimation. The blue dashed line represents the length of the projection of T-R distance on the perpendicular axis out of the receiver,  $D_p$ . The red dotted line represents the horizontal T-R distance,  $D_h$ , to the right tail light.

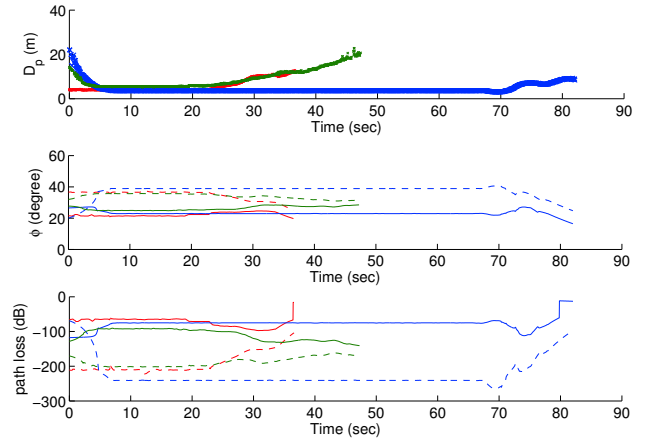


Fig. 5. Examples of the obtained vehicle traces:  $D_p$ ,  $\phi$ , and  $H(0)$ , in different colors. Top: solid lines - after outlier removal; crosses - original data. Middle and bottom: dash lines - left tail light; solid lines - right tail light.

$D_v$  is assumed to be 0.5 meter. Then, we have  $W_R = w_R \epsilon$ ,  $\phi_R = \tan^{-1}(\frac{W_R}{D_p})$ ,  $D_h = \sqrt{D_p^2 + W_R^2}$ , and  $D = \sqrt{D_h^2 + D_v^2}$ <sup>2</sup>. Then the path loss can be calculated with Eq. 1.

## IV. RESULTS

Results presented in this section are calculated from 158 mobility traces obtained from the video files, after dropping traces with less than 10 image frames with detected tail lights or traces with less than 30% image frames with detected tail lights. The video files are collected by a dashboard camera mounted behind the windshield of a passenger car driven in the urban area of Taipei. Before these traces are used for the calculation of path loss, we used local regression with weighted linear least squares and a 1st degree polynomial model to remove the outliers in the time functions of  $D_p$ ,  $W_L$ ,

<sup>2</sup>Parameters related to the left tail light is obtained similarly.

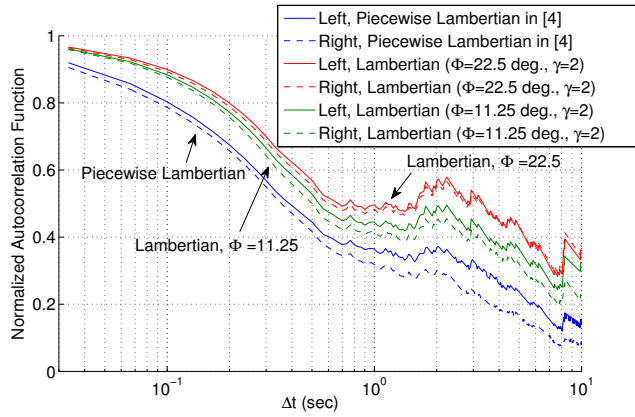


Fig. 6. Normalized Autocorrelation Function

$W_R$ , etc. Fig. 5 shows the time functions of  $D_p$ ,  $\phi$ , and  $H(0)$ , of one of the longer obtained traces. Note that the variation of path loss could be as large as to 25 dB.

The path loss values used in this section are calculated with three different light models: a piecewise Lambertian model based on real-world measurements of an automotive tail light [4] (with plastic lens and reflectors to regulate the optical radiation within a small angle), and two regular Lambertian models (i.e., a bare optical source) that have different view angles, with half-power angles  $\Phi_{1/2}$  of 22.5 and 11.25 degrees<sup>3</sup>, respectively.

Autocorrelation function and coherence time are often used to indicate the level of time variation caused by fading. Fig. 6 shows the obtained average normalized autocorrelation function of the path loss  $R_{H(0)}(\Delta t)$ . One can observe that the left tail light generally has a higher autocorrelation value than its right counterpart, due to the fact that the car is driven on the right; the variation of  $\phi'$  of the left tail light is usually smaller as it can go to neither the left side of the road nor the very right side of the road. One can also observe that, the piecewise Lambertian model has the smallest autocorrelation, as a real-life LED tail light radiates optical energy within a small angle and changes of  $\phi'$  due to vehicle mobility result in more fluctuation in path loss values. As shown in Table I, when the optical power is radiated with a larger half-power angle (beam angle), the coherence time is improved. The 50% coherence time of a V2LC link, considering only fading caused by vehicle mobility, is on the order of hundreds of milliseconds while the 90% coherence time is on the order of tens of milliseconds (see Table I). This is at least an order larger than the values reported in V2V RF channel, which range from 0.45 ms to 5.31 ms in the urban scenarios [8].

## V. CONCLUSION AND FUTURE WORK

In this paper, we took the first look at channel fading of a V2LC link caused by vehicle mobility. Utilizing video data collected from a dashboard camera mounted behind the

<sup>3</sup>Chosen based on the automotive regulation that states the tail lights need to have an angle of geometric visibility of 45 degrees.

TABLE I  
COHERENCE TIME COMPARISON (SECOND)

Light model	Left tail light		Right tail light	
	$T_{c,0.9}$	$T_{c,0.5}$	$T_{c,0.9}$	$T_{c,0.5}$
Piecewise Lambertian	0.033	0.367	0.033	0.333
Lambertian, $\Phi_{1/2} = 11.25^\circ$	0.067	0.667	0.067	0.600
Lambertian, $\Phi_{1/2} = 22.5^\circ$	0.067	0.533	0.067	0.500

$T_{c,0.9}$ : 90% coherence time;  $T_{c,0.5}$ : 50% coherence time

windshield of a driven vehicle, we applied computer vision techniques to detect neighboring vehicles and estimate their relative locations. The estimated location parameters are then used to calculate the path loss of a V2LC link and its time variation, with the assumption that the tail lights of the detected vehicle were transmitting V2LC signals. Our results show that V2LC links have much slower time variation; the coherence time of a V2LC link ranges from tens of milliseconds to hundreds of milliseconds, which is at least an order larger than that of RF V2V. Our future works include collecting and processing a larger amount of data from different driving scenarios, and performing V2LC received power measurements to validate that the proposed approach of using the video data is sufficiently accurate. We also plan to investigate other aspects of V2LC channel fading with the obtained data, such as outage probability and fade duration.

## ACKNOWLEDGMENT

This work is supported in part by Ministry of Science and Technology, National Taiwan University and Intel Corporation under grants MOST-102-2911-I-002-001, MOST-102-2221-E-002-093-MY2, and NTU-103R7501.

## REFERENCES

- [1] Y. Fujii, W. Strijbosch, O. Vogler, F. Wunderlich, and D. Wee, "Chain lighting: Charting the evolving automotive LED value chain," McKinsey & Company, Inc., 2010. [Online]. Available: <http://autoassembly.mckinsey.com>
- [2] S.-H. Yu, O. Shih, N. Wisitpongphan, H.-M. Tsai, and R. D. Roberts, "Smart automotive lighting for vehicle safety," *IEEE Communications Magazine*, vol. 51, no. 12, pp. 50–59, December 2013.
- [3] Y. Morgan, "Notes on DSRC and WAVE standards suite: Its architecture, design, and characteristics," *IEEE Communications Surveys and Tutorials*, vol. 12, no. 4, pp. 504–518, 2010.
- [4] W. Viriyasitavat, S.-H. Yu, and H.-M. Tsai, "Short paper: Channel model for visible light communications using off-the-shelf scooter taillight," in *Proc. IEEE Vehicular Networking Conference (VNC)*, December 2013, pp. 170–173.
- [5] P. F. Felzenszwalb, R. B. Girshick, and D. McAllester, "Cascade object detection with deformable part models," in *Proc. IEEE conference on Computer vision and pattern recognition (CVPR)*, 2010, pp. 2241–2248.
- [6] O. Ronan, J. Edward, and G. Martin, "Rear-lamp vehicle detection and tracking in low-exposure color video for night conditions," *IEEE Transactions on Intelligent Transportation Systems*, vol. 11, no. 2, pp. 453–462, 2010.
- [7] A. Mihael, B. Markus, K. Hans-Peter, and J. S., "Optics: Ordering points to identify the clustering structure," in *Proc. ACM international conference on Management of data (SIGMOD)*, vol. 28, no. 2, 1999, pp. 49–60.
- [8] C. F. Mecklenbrauker, A. F. Molisch, J. Karedal, F. Tufvesson, A. Paier, L. Bernado, T. Zemen, O. Klemp, and N. Czink, "Vehicular channel characterization and its implications for wireless system design and performance," *Proceedings of the IEEE*, vol. 99, no. 7, pp. 1189–1212, 2011.